BMC Nephrology

RESEARCH

Open Access

Neutrophil extracellular traps-related genes contribute to sepsis-associated acute kidney injury

Tang Shaoqun[1†], Yu Xi[1†], Wang Wei[1†], Luo Yaru[1], Lei Shaoqing[1], Qiu Zhen[1], Yang Yanlin[1], Sun Qian[1*] and Xia Zhongyuan[1*]

Abstract

Background Neutrophil extracellular traps (NETs) and oxidative stress (OS) may be involved in sepsis-associated acute kidney injury (SA-AKI). The aim of this study was to identify potential regulators which modulate NETs and OS in SA-AKI, and to find potential therapeutic agents.

Methods and Materials SA-AKI-related datasets GSE255281 and GSE225192 were downloaded from Gene Expression Omnibus. Molecular subtypes associated with NETs were identified by unsupervised clustering. The OS-related genes were obtained by weighted gene co-expression network analysis. Differentially expressed genes were screened by "limma" package in R. Least absolute shrinkage and selection operator algorithm was applied to identify the hub genes. Additionally, the biological functions of the hub genes were analyzed with single sample gene set enrichment analysis. NetworkAnalyst database was searched to screen the drugs targeting the hub targets. qRT-PCR was used to analyze the expression of key genes in the peripheral blood mononuclear cells (PBMCs) of the patients with SA-AKI and healthy controls. HK-2 cells and human umbilical vein endothelial cells (HUVECs) were induced by lipopolysaccharide (LPS) to construct a SA-AKI model, and the effects of estradiol and (+)-JQ1 on HK-2 cells and HUVECs were evaluated by CCK-8 assays, flow cytometry and OS indices.

Results Based on NETs-related genes, SA-AKI samples could be divide into two subgroups, and the differentially expressed genes between two subgroups were associated with OS. In silico analyses identified 13 hub targets. The expression of ECT2 and CHRDL1 in PBMCs of SA-AKI patients was significantly lower than that in control group, and the expressions of PTAFR, CSF3 and FOS were significantly higher. Estradiol and (+)-JQ1, which targeted more of the hub targets with good binding affinity, could increase the viability of HK-2 cells and HUVECs induced by LPS and inhibit apoptosis and OS.

Conclusion Formation of NETs, contributes to OS and pathogenesis of SA-AKI. Estradiol and (+)-JQ1, targeting multiple regulators in the formation of NETs, may be potential therapeutic agents for the treatment of SA-AKI.

†Tang Shaoqun, Yu Xi and Wang Wei shared as co-first authors.

*Correspondence:
Sun Qian
queenie_sun@whu.edu.cn
Xia Zhongyuan
xiazhongyuan2005@aliyun.com

Full list of author information is available at the end of the article

Clinical trial number Not applicable.

Keywords Sepsis, Renal injury, Neutrophil extracellular traps, Oxidative stress

Introduction

Sepsis is a life-threatening clinical syndrome characterized by organ dysfunction due to the patient's dysregulated response to infection [1, 2]. Sepsis is associated with high mortality and morbidity, resulting in a heavy social burden worldwide [3]. Acute kidney injury (AKI) caused by sepsis is a common complication in hospitalized and critically ill patients, and up to 60% of sepsis patients suffer from AKI [4]. Sepsis-associated acute kidney injury (SA-AKI) can increase the risk of death and longer hospital stay [5, 6]. Therefore, exploring the biological mechanism of SA-AKI and identifying biomarkers of SA-AKI are crucial for the early diagnosis of patients and the development of targeted therapeutic drugs.

Neutrophils belong to the first line of innate immunity against pathogens. In the early stages of sepsis, neutrophils recruit to the site of infection, and release reactive oxygen species (ROS), reactive nitrogen species (RNS), and neutrophil extracellular traps (NETs) to kill pathogens [7]. NETs are the "net" of DNA, histone proteins and antimicrobial peptides produced by active neutrophils, which can trap and kill pathogens such as bacteria, fungi and viruses and play an important role in innate immunity [8, 9]. However, NETs are a "double-edged sword", and excessive NETs lead to severe inflammation [10], apoptosis [11], thrombosis [12], and organ dysfunction [13, 14]. The severity of infant sepsis is positively correlated with the level of NETs [15]. In the SA-AKI mouse model, NETs formation is significantly increased, and blocking NETs formation can significantly reduce mortality and ameliorate AKI in mice [16, 17]. Therefore, elucidating the molecular mechanisms by which NETs formation guide host defense against SA-AKI is helpful in developing potential strategy for SA-AKI treatment.

Oxidative stress (OS) is considered to be the main factor to accelerate SA-AKI progression. ROS and RNS mediate abnormal renal microcirculation, local tissue hypoxia and mitochondrial dysfunction [18]. In addition, enhanced OS is a key mediator of innate immune response and can cause a "cytokine storm" that aggravates kidney injury [19]. Increasing studies support that antioxidants may be potentially effective drugs for the treatment of SA-AKI [20, 21].

Increasing studies have supported that NETs formation contributes to the activation of inflammatory cascade, leading to increased OS and aggravated organ injury [22, 23]. However, there were few studies focusing on the relationship between NETs formation and OS in the pathogenesis of SA-AKI. In the present work, based on bioinformatics analysis, we report that formation of NETs, probably contributes to OS in the pathogenesis of SA-AKI, and potential drugs for treating SA-AKI are preliminarily screened.

Materials and methods

Overall design of the present work

In this study, SA-AKI samples of mice were classified into two subtypes using unsupervised clustering based on NETs-related genes. The two subtypes also showed different OS status. Based on OS-related genes, OS-related gene modules were obtained by weighted gene co-expression network analysis (WGCNA). Subsequently, differentially expressed gene (DEG) analysis was performed on SA-AKI samples and control samples. Least absolute shrinkage and selection operator (LASSO) was used to further screen the hub genes from the genes in the intersection. The predictive value of hub genes for SA-AKI was analyzed by using the nomogram and receiver operator characteristic (ROC) curve. Next, bioinformatics analysis, molecular docking and in vitro assays were performed to explore the role of hub genes in SA-AKI pathogenesis, and evaluate their potential as drug targets. The work flow of the present work is shown in Fig. 1.

Data collection and data processing

In Gene Expression Omnibus (GEO) database (http://www.ncbi.nlm.nih.gov/geo), "SA-AKI" was used as the key work to search the datasets, and GSE255281 and GSE225192 datasets were downloaded after filtering. A total of 65 SA-AKI samples of C57/BL6 mouse constructed by cecal ligation and puncture (CLP) or lipopolysaccharide (LPS) induction, and 60 samples of sham group were obtained. "comBat" function in the R package "sva" [24] was used to merge two datasets and eliminate batch effects, which was validated by principal component analysis (PCA). The basic information and the links of the datasets are shown in Table 1.

Analysis of NETs-related subtypes

57 homologous NETs-related genes were obtained from a previously published study [25], and R package "ConsensusClusterPlus" [26] was used to classify all SA-AKI samples based on these genes based on k-means algorithm and euclidean distance. Through the analysis of consensus cumulative distribution function (CDF) and Delta area plots, finally, the clustering number $k = 2$ was determined as the ideal value.

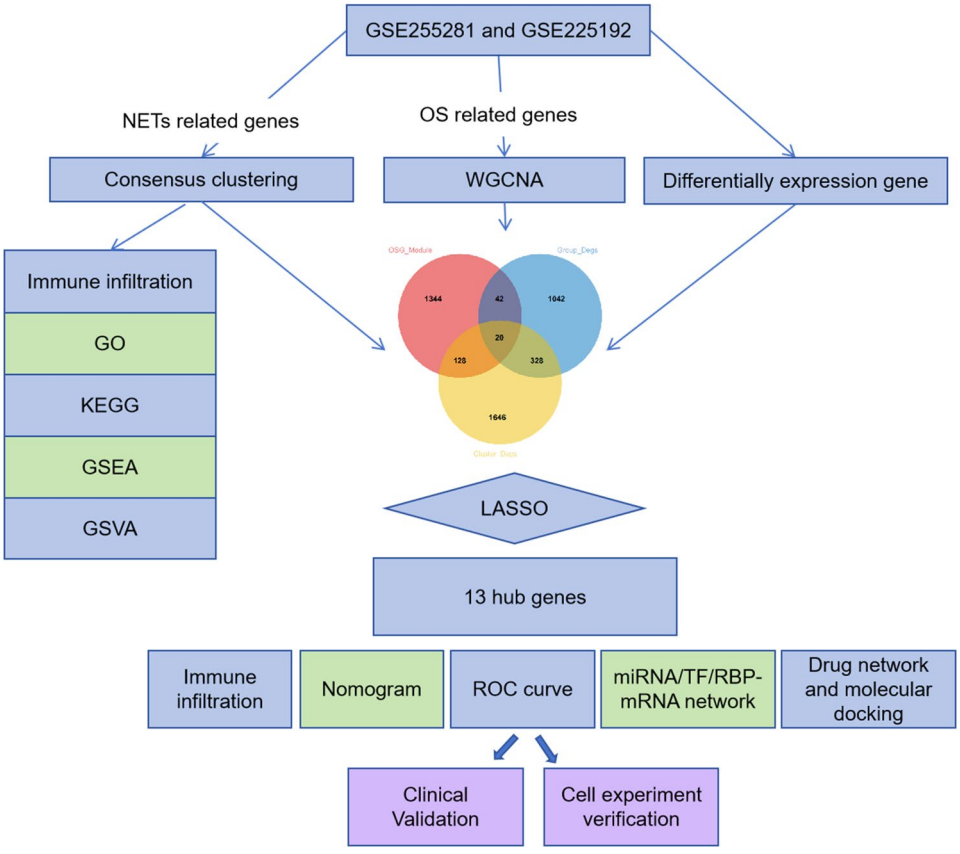

Fig. 1 Work flow of the present work

Table 1 The information of the datasets used in the present study

Dataset	Experimental design	Platform	Link
GSE255281	10–14 week old C57BL/6J mice were treated with LPS (8 mg/kg bw) ($n=5$) and kidneys collected after 24 h for RNA-sequencing.	GPL21493, Illumina HiSeq 3000 (Mus musculus)	https://www.ncbi.nlm.nih.gov/geo/query/acc.cgi?acc=GSE255281
GSE225192	Cecal ligation & puncture (CLP) was performed to induce sepsis of C57BL6/OlaHsd mice ($n=60$). The mice in sham-operated group ($n=60$) were used as the controls. Kidney cortex tissues (arterioles, glomeruli, peritubular capillaries, post-capillary venules) were collected for RNA sequencing.	GPL21103 Illumina HiSeq 4000 (Mus musculus)	https://www.ncbi.nlm.nih.gov/geo/query/acc.cgi?acc=GSE225192

DEG analysis

R package "limma" [27] was used for DEG analysis. The thresholds of DEGs were fold change (FC) ≥ 1.5 and P value < 0.05. The volcano map and heat map were drawn using R packages "ggplot" and "pheatmap" [28, 29].

WGCNA

All SA-AKI samples were analyzed using the R package "WGCNA" [30], and the soft threshold was set as 4. Topological overlap matrix (TOM) was used to infer the network connection level. Next, hierarchical clustering was used to build a tree diagram to calculate the correlation between module characteristic genes and disease phenotypes. OS-related genes were obtained from GeneCards database (https://www.genecards.org/) [31], and single sample gene set enrichment analysis (ssGSEA) [32] was performed to evaluate the OS status of each sample, and the scores were used as the traits. The genes in the key modules ($r>0.3$, $P<0.05$) were considered to be the crucial genes associated with OS in SA-AKI.

Functional enrichment analysis

Gene ontology (GO) and Kyoto Encyclopedia of Genes and Genomes (KEGG) functional enrichment analyses were performed using R package "ClusterProfiler" [33] (p.adjust < 0.05). GO included biological processes (BP), cellular components (CC), and molecular functions (MF). Gene set variation analysis (GSVA) was performed with R package "GSVA" [32], based on GO-BP gene set and Reactome gene set, which were downloaded from MSigDB database [34], to assess potential biological functional changes in different samples. Gene set

enrichment analysis (GSEA) was performed using the R package "clusterProfiler" to observe the differential pathways between subtypes. Mouse HALLMARK gene set was downloaded from MSigDB database [34], and then HALLMARK gene set score was calculated for all samples using ssGSEA algorithm [32], and a heat map was drawn to show the difference of HALLMARK scores among different groups. Spearman method was used to calculate the correlation between hub genes and HALLMARK pathways.

Screening of hub genes

LASSO algorithm [35] was used to conduct cross-validation based on the expression data of genes in the intersection, and lambda.1se was selected as the final lambda coefficient to obtain 13 key genes of the model. Subsequently, the 13 genes were analyzed with Spearman correlation analysis and differential expression analysis.

Construction and verification of nomogram

Based on the hub genes, the R package "rms" [36] was applied to construct a nomogram to predict the possibility of SA-AKI, and a calibration curve was drawn to test the reliability of the nomogram. The area under the curve (AUC) was then calculated to further evaluate the predictive value of the nomogram for diagnosing SA-AKI [37, 38]. AUC > 0.7 was considered as the ideal predictive value.

Drug screening

NetworkAnalyst database [39] was applied to predict the drugs targeting the hub targets. Candidate drugs that targeted 5 or more hub targets were collected. Toxic drugs were further excluded based on literature reviewing, and finally 3 candidate drugs were obtained. From the CTD database (http://ctdbase.org/) [40] and the PubChem database (https://pubchem.ncbi.nlm.nih.gov/), the secon dary structures of the drugs (SDF file) were downloaded. The structures of hub targets (mol2 file) were downloaded from the Uniprot database (https://uniprot.org/) [41]. The structure files were then preprocessed with the AutoDock software, and AutoDock Vina software (version: 1.5.7) [42] was used for molecular docking, and the PyMol software (version: 2.4.0) [43] was used to visualize the results. Binding affinity <-5 kcal/mol suggested that the compound could bind with the target.

Clinical sample collection

This study collected 22 patients with septic kidney injury from the Intensive Care Unit of Renmin Hospital of Wuhan University from January 2022 to December 2023. All patients met the following inclusion criteria: (1) aged between 18 and 90 years; (2) diagnosed with sepsis [44] and AKI in stage 2 of KDIGO classification [45]. Patients with a history of chronic kidney disease (chronic renal failure due to glomerulonephritis, diabetic nephropathy, hypertensive nephropathy, hereditary nephritis, and a variety of other conditions), multiple hospitalizations, and ICU stays of less than 24 h (suggesting the patient's condition was speedily improving or declining, and the samples may not reflect the true condition of SA-AKI) were excluded. Blood samples of these patients, and 15 healthy controls from the Physical Examination Center were collected, and peripheral blood mononuclear cells (PBMCs) were obtained according to density differences in accordance with previous methods [46, 47]. This study was performed in accordance with the Declaration of Helsinki. Considering the information of the patients were not released during the study, and the study didn't change the procedures of the diagnosis and treatment, and this study was exempted by the Ethics Committee of Renmin Hospital of Wuhan University, and the formal vote was exempted.

Cell culture

Human renal proximal tubular epithelial cell line HK-2, and human umbilical vein endothelial cells (HUVECs) were obtained from the Cell Bank of the Committee for the Preservation of Collections and Cultures of Chinese Academy of Sciences (Shanghai, China). The cells were cultured in RPMI-1640 medium (Invitrogen, Shanghai, China) containing 10% fetal bovine serum (FBS, Invitrogen, Shanghai, China), 100U/mL penicillin and 0.1 mg/mL streptomycin (Invitrogen, Shanghai, China), in an incubator (37℃, 5% CO_2). LPS (1 μg/ml) (Beyotime, Shanghai, China) was used to stimulate HK-2 cells and HUVECs to construct the in vitro model of SA-AKI. After treatment with 100 nM estradiol or (+)-JQ1 compound (Beyotime, Shanghai, China), HK-2 cells and HUVECs were then treated with LPS for 22 h [48].

Quantitative reverse transcription-polymerase chain reaction (qPCR)

Total RNA, extracted with TRIzol reagent (Invitrogen, Shanghai, China), was reverse-transcribed into cDNA using a PrimeScript™ RT kit (Takara, Dalian, China). qPCR was performed using TB Green™ Premix Ex Taq™ kit (Takara, Dalian, China), primers and cDNA on the ABI 7300 Sequence Detection System (Applied Biosystems, Foster City, CA, USA). The condition of qPCR: denaturation at 95 °C for 3 min, 40 cycles of 95 °C for 12s, 62 °C for 12s, and then extended at 62 °C for 40 s. GAPDH served as an internal control for calculating mRNA expression levels. The primer information is shown in Table 2.

Table 2 Primer sequences used in the present study

gene	Forward primer (5′→3′)	Reverse primer (5′→3′)
CCDC159	TGAACAGGTGAAGCCCTTGG	ACTCGAAAGCCTTGGTCTGG
ECT2	ACTACTGGGAGGACTAGCTTG	CACTCTTGTTTCAATCTGAGGCA
CHRDL1	CCCAGACTCCTTACCCCCA	GGAACAGAGACTGGGAAGGC
FOS	GGAGGGAGCTGACTGATACAC	AGCTGCCAGGATGAACTCTAG
INHBB	CCTGAAACTCCTGCCCTACG	CCACCATGTTCCACCTGTCA
CSF3	GAGAAGCTGGTGAGTGAGGCAG	TAGAACGCGGTACGACACCT
FHAD1	TTTTGGAGACTGTGGGGAGA	ATCATGACCCAACGTGGACC
PTAFR	CGAGAAGCCGTCCAGGAAAC	GCCTCAGCCTCTATGCTGTC
GAPDH	TTTTGCGTCGCCAGCC	ATGGAATTTGCCATGGGTGGA

Cell viability assay

The Cell Counting Kit-8 (CCK-8) test Kit (Beyotime, Shanghai, China) was used to detect cell viability. In short, HK-2 cells and HUVECs were added to 96-well plates with a density of 6×10^3 cells / well and cultured for 24 h. After that, 10 μL CCK-8 solution was added to each well and the cells were incubated for 2 h. Finally, the absorbance of the samples was measured with a microplate reader (Invitrogen, Shanghai, China) at 450 nm wavelength.

Flow cytometry

An Annexin V-FITC/propidiumiodide (PI) Apoptosis Detection Kit (Yeasen Biotech, Shanghai, China) was used to detect the apoptosis of HK-2 cells and HUVECs. HK-2 cells and HUVECs were pre-cooled and washed with phosphate buffer saline twice, and then resuspended with 1×binding buffer. The cell suspension was added with 5 μL AnnexinV-FITC and 5 μL PI, thoroughly mixed and incubated at room temperature for 15 min. After washing with binding buffer, the apoptosis rate of the cells was detected by a flow cytometer (Attune NxT, Thermo Fisher, USA).

Detection of ROS and malondialdehyde (MDA)

The ROS and MDA contents in HK-2 cells and HUVECs were detected according to the manufacturer's instructions of the corresponding ROS and MDA detection kits (Beyotime, Shanghai, China).

Statistical analysis

Data processing and analysis were performed in the R software (version: 4.3.3) and GraphPad Prism software (version: 8.2.1). The continuous variables with normal distribution were represented by "mean ± standard deviation (SD)" and compared by independent student t tests or one-way ANOVA. Non-parametric test was used for variables that did not conform to normal distribution. Spearman correlation analysis was used to analyze the correlation. A P value < 0.05 was considered statistically significant.

Results

Classification of NETs-related subtypes in SA-AKI

First of all, GSE255281 and GSE225192 datasets were merged, and the batch effect was removed (Supplementary Fig. 1A&B). The merged dataset contained a total of 65 SA-AKI samples and 60 sham control (Sham) samples. Based on 57 NETs-related genes, two subtypes of SA-AKI were obtained using k-means algorithm. Subtype 1 contained 52 samples, and subtype 2 contained 13 samples (Fig. 2A). Between the two subgroups, a total of 2122 DEGs were identified (Fig. 2B), and the expression profiles of the top 10 up-regulated and down-regulated genes in the two subgroups are shown in a heat map (Fig. 2C). GO analysis showed that DEGs were mainly associated with regulation of inflammatory response, regulation of cell-cell adhesion, positive regulation of response to external stimulus, protein serine/threonine kinase activity, etc. (Fig. 2D). KEGG enrichment analysis suggested that the DEGs were mainly associated with inflammatory signaling pathways, including MAPK signaling pathway, NF-κB signaling pathway and TNF signaling pathway (Fig. 2E). Differences between biological processes and signaling pathways between the two subtypes were further analyzed by GSEA and GSVA. GSEA showed smooth muscle contraction, DNA recombination, protein localization to cell junction, oxidative phosphorylation, respiratory electron transport, detoxification of reactive oxygen species, and mitochondrial biogenesis were differentially enriched in the two subtypes (Fig. 3A-B). GSVA showed that biological processes such as amino acid metabolism, lipid metabolism, heme degradation, glutathione synthesis and recovery, and peroxisomal lipid metabolism were differentially enriched in the two subtypes (Fig. 3C-D). These results suggest that NETs in SA-AKI are probably related to OS.

Identification OS-related genes associated with NETs formation in SA-AKI

Next, we tried to screen the regulators of OS during SA-AKI. Between SA-AKI and sham samples, there were 1432 DEGs (Fig. 4A-B). WGCNA was also performed, with the OS status, which were obtained by ssGSEA, as the traits. Suitable soft threshold $\beta = 4$ was screened (Fig. 4C). 17 gene modules were obtained by WGCNA (Fig. 4D), and MEbrown and MEroyalblue modules were remarkably associated with OS ($r > 0.3$ and $P < 0.05$) (Fig. 4E). Subsequently, 20 genes in the intersection of the genes in MEbrown and MEroyalblue modules, DEGs between SA-AKI samples and Sham samples, and DEGs between the two subgroups of SA-AKI were obtained (Fig. 4F). GO analysis showed that these 20 genes were

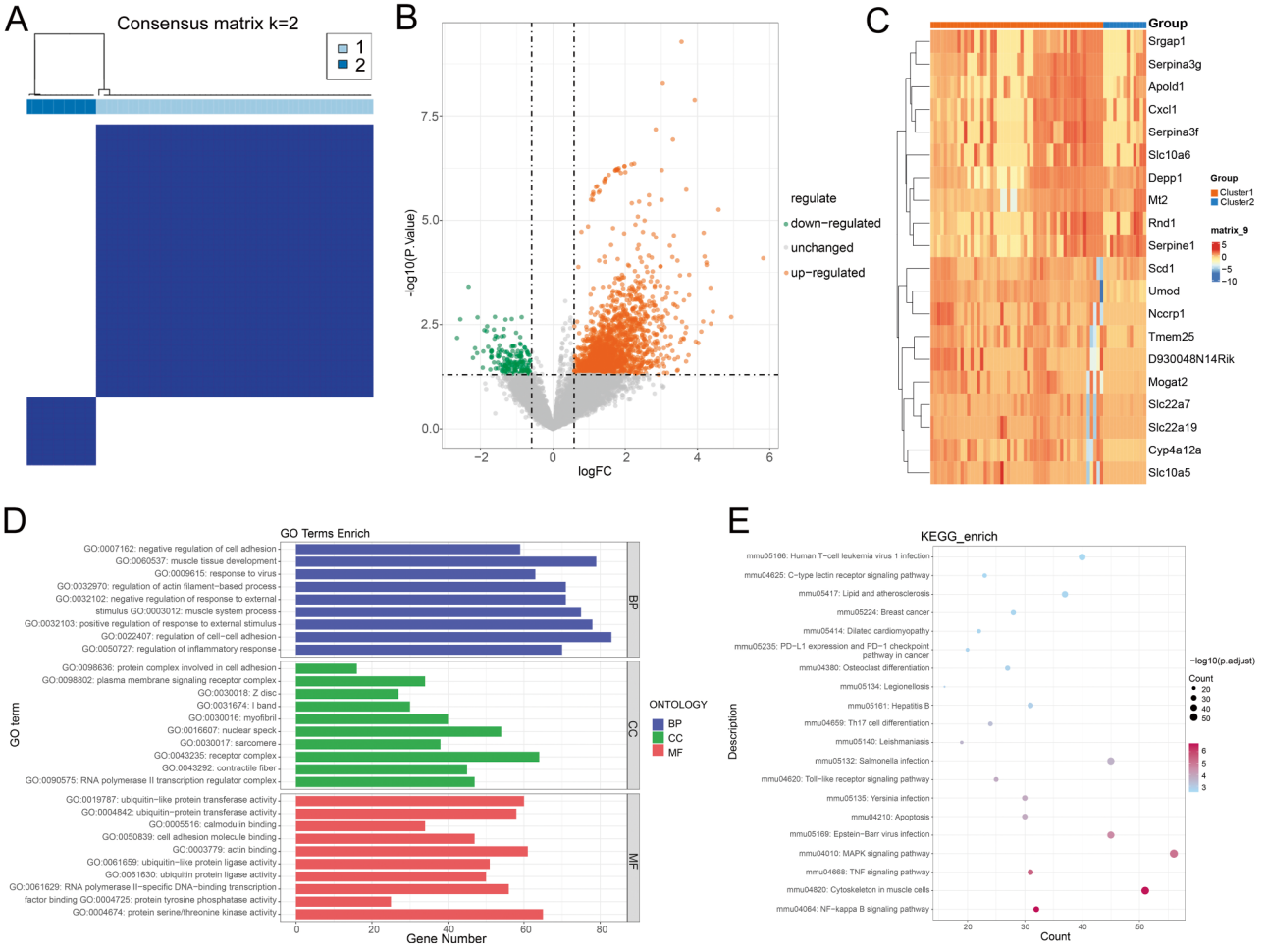

Fig. 2 Classification of NETs-related subtypes of SA-AKI samples in GSE255281 and GSE225192. (**A**) Based on 57 NETs-related genes, two subtypes of SA-AKI were obtained using k-means algorithm. (**B**) The volcano map of the results of differentially expressed genes (DEGs) between two NETs-related subgroups. (**C**) The heat map of top 10 DEGs with up-regulated or down-regulated expression in the two subgroups. (**D**) The bar chart showing the top 10 items of biological process (BP), cellular component (CC) and molecular function (MF) associated with the DEGs in GO analysis. (**E**) The bubble map of the top 20 items of KEGG enrichment analysis based on the DEGs

associated with cellular response to leptin stimulus, response to leptin and cellular response to reactive oxygen species (Fig. 4G). KEGG enrichment analysis showed that these genes were involved in regulating apoptosis, cAMP signaling pathway, etc. (Fig. 4H).

Identification of hub genes involved in regulating NETs and OS during SA-AKI

In order to further identify hub genes from the 20 genes mentioned above, LASSO algorithm was used (Fig. 5A-B), and 13 hub genes were obtained. They were *Ccdc159*, *Abtb3*, *Ect2*, *Chrdl1*, *Gm11434*, *6030443J06Rik*, *Gm43860*, *Gm3953*, *Fos*, *Inhbb*, *Csf3*, *Fhad1*, and *Ptafr*. Among them, in the SA-AKI samples, *Ccdc159*, *Abtb3*, *Ect2*, *Chrdl1*, *Gm11434*, *6030443J06Rik*, *Gm43860* and *Gm3953* were lowly expressed; while *Fos*, *Inhbb*, *Csf3*, *Fhad1*, and *Ptafr* were significantly overexpressed (Fig. 5C). Correlation analysis showed that most of these 13 genes showed significant positive correlation, indicating that these 13 genes jointly play a role in the formation of NETs and promoting OS during SA-AKI (Fig. 5D). Next, a nomogram was constructed based on the 13 genes (Fig. 5E). Calibration curve showed the nomogram had good ability to predict SA-AKI (Fig. 5F). Then ROC curve was used to investigate the ability of hub genes to predict the occurrence of SA-AKI. The results showed that AUC of all 13 hub genes was greater than 0.7, indicating that these 13 genes had a good predictive ability for the occurrence of SA-AKI (Fig. 5G). Compared with single genes, the nomogram had better predictive value (AUC = 0.910) (Fig. 5H). These results suggest that these 13 hub genes, which are associated with the formation of NETs and OS, are involved in the pathogenesis of SA-AKI, and they are potential biomarkers and drug targets of SA-AKI.

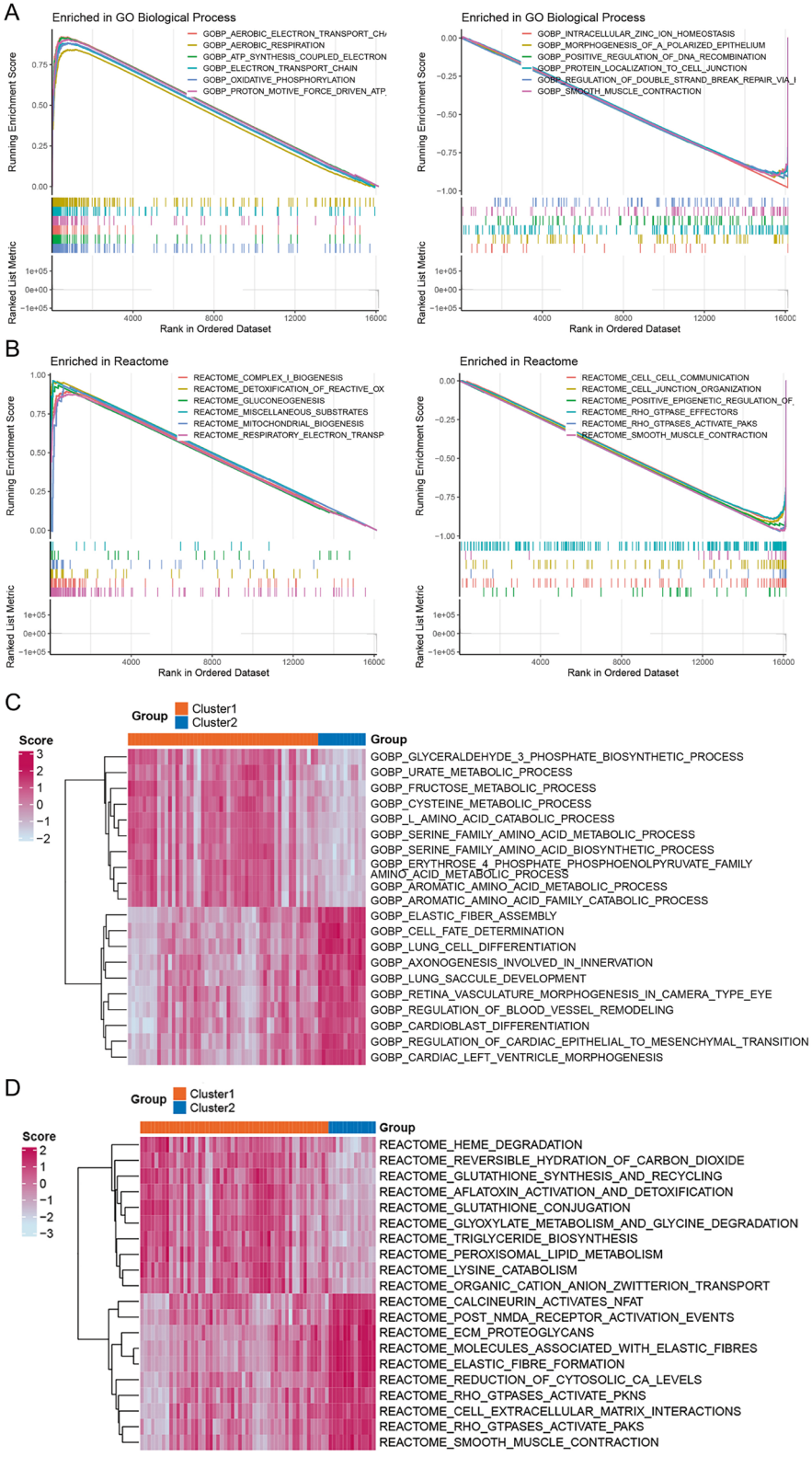

Fig. 3 Biological process differences between NETs-related subtypes in SA-AKI. (**A**) Biological process (BP) differences between the two subtypes were analyzed by gene set enrichment analysis (GSEA) based on GO Biological Process gene set. (**B**) BP differences between the two subtypes were analyzed by GSEA based on the Reactome gene set. (**C**) BP differences between the two subtypes were analyzed using gene set variation analysis (GSVA) based on GO Biological Process gene set. (**D**) BP differences between the two subtypes were analyzed by GSVA based on the Reactome gene set

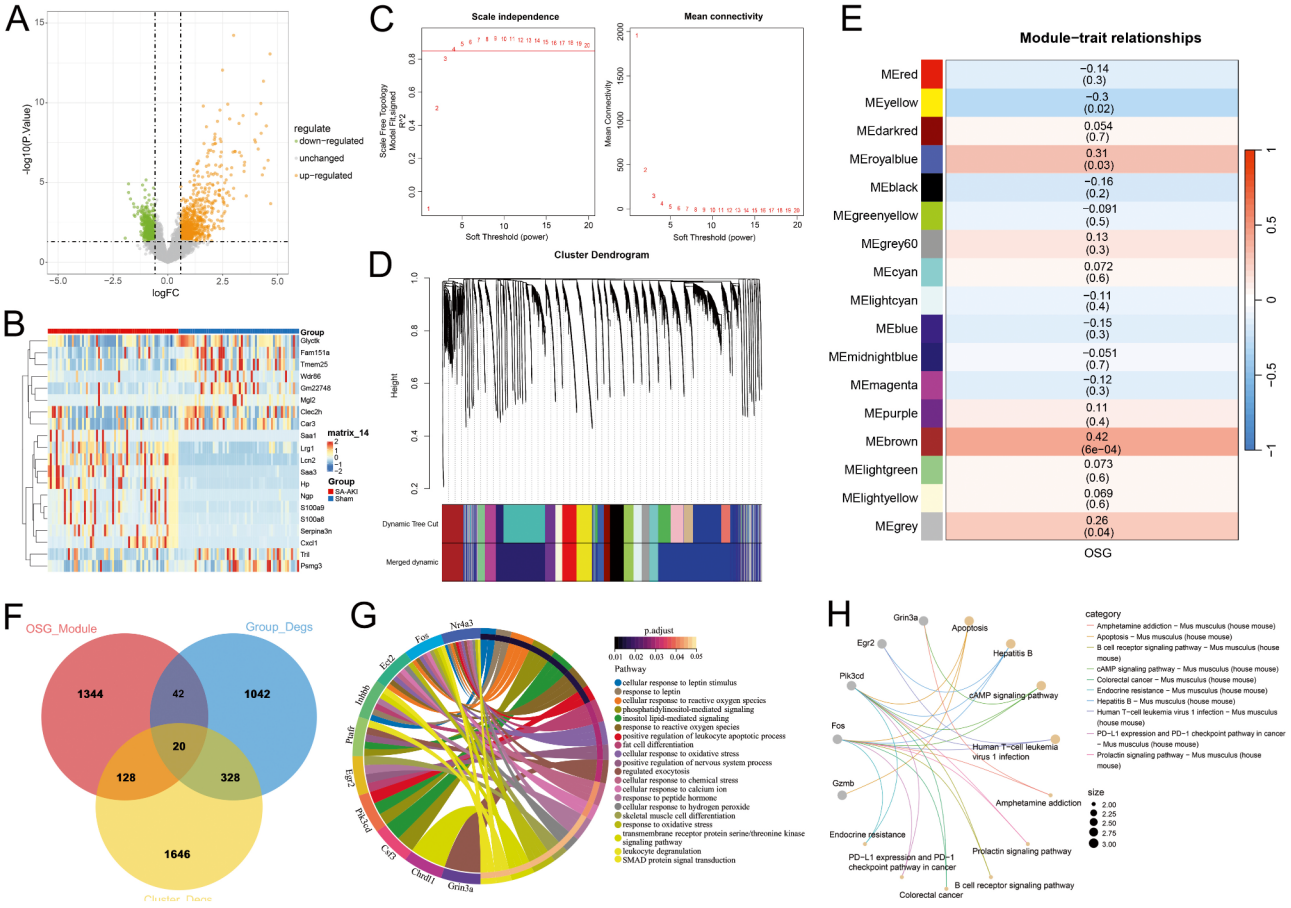

Fig. 4 Identification and enrichment analysis of NETs-related oxidative stress (OS) genes. (**A**) The volcano map showing the differentially expressed genes (DEGs) between SA-AKI samples and sham samples. Orange represents the significantly up-regulated gene, green represents the significantly down-regulated gene, and gray represents a gene with insignificant. (**B**) The heat map showing the top 10 up-regulated and top 10 down-regulated DEGs between SA-AKI and Sham samplesexpression difference. (**C**) Scale independence and average connectivity plots are used to select the best soft threshold for weighted gene co-expression network analysis (WGCNA). (**D**) The clustering tree of gene clusters in WGCNA. (**E**) The heat map showing the correlation between gene modules and ssGSEA scores of OS. (**F**) A venn diagram was used to obtain the genes in the intersection of the genes in MEbrown and MEroyalblue modules (OSG_module), DEGs between SA-AKI samples and Sham samples (Groups_Degs), and DEGs between the two subgroups of SA-AKI (Cluster_Dges). (**G**) String diagram of the top 20 items of GO analysis based on the genes in the intersection. (**H**) String diagram of the top 10 items of KEGG enrichment analysis based on the genes in the intersection

In silico analysis of the biological functions of the 13 hub genes

Based on the mouse HALLMARK gene set, functional enrichment analysis showed that grouping of SA-AKI samples and the expression level of the 13 hub genes were associated with multiple inflammation-related pathways including TNF-α signaling, NF-κB signaling, IL6-JAK-STAT3 signaling, etc. (Fig. 6A,B). ssGSEA was then applied to perform immunoinfiltration analysis, and it showed that type 17 T helper cell, regulatory T cell, gamma delta T cell, central memory CD8 T cell, activated dendritic cell, macrophage, activated CD4 T cell, and myeloid derived suppressor cell showed significant differences between SA-AKI and sham samples (Fig. 6C). Correlation analysis showed that the infiltration of regulatory T cell was significantly negatively correlated with *Ccdc159* and *Abtb3*; infiltration of macrophage was significantly negatively correlated with *Ccdc159*, *Gm3953* and *Abtb3*; infiltration of myeloid derived suppressor cell was significantly positively correlated with *Fos*, *Csf3* and *Ptafr*; and infiltration of activated dendritic cell was significantly positively correlated with *Csf3* and *Ptafr*; infiltration of activated CD4 T cell was significantly positively correlated with *Csf3* and *Inhbb*, and negatively correlated with *Ccdc159* (Fig. 6D). Notably, neutrophil infiltration was significantly positively correlated with 9 hub genes (Fig. 6D).

Results of drug prediction and molecular docking

Subsequently, 415 drugs targeting hub targets were obtained through NetworkAnalyst database (Fig. 7A), and 6 compounds targeted at least 5 hub targets, including acetaminophen, silicon dioxide, estradiol, aflatoxin B1, potassium chromate (VI) and (+)-JQ1 (Table 3).

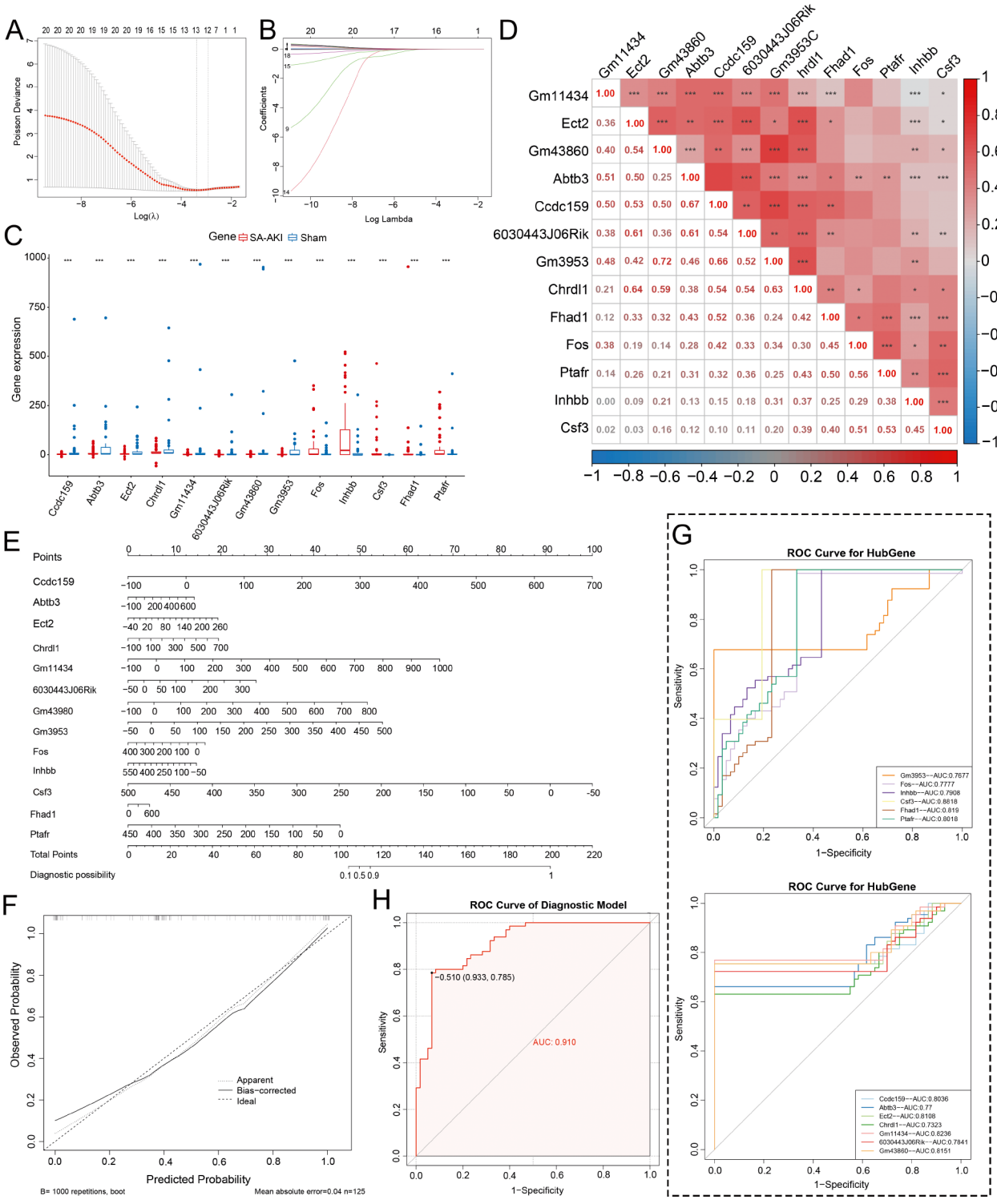

Fig. 5 Identification of hub genes related with formation of NETs and OS in SA-AKI. (**A**-**B**) The hub genes were obtained by least absolute shrinkage and selection operator (LASSO) and 10-fold cross-validation. (**C**) The box plot of hub gene expression in SA-AKI and sham samples. (**D**) Correlation analysis between hub genes in SA-AKI samples. (**E**) A nomogram based on the 13 hub genes predicting the occurrence of SA-AKI. (**F**) Calibration curves to assess the predictive efficacy of the nomogram. (**G**) Receiver operator characteristic (ROC) curves of hub genes for diagnosing SA-AKI. (**H**) ROC curve of the nomogram for diagnosing SA-AKI. *$P < 0.05$, **$P < 0.01$, ***$P < 0.001$

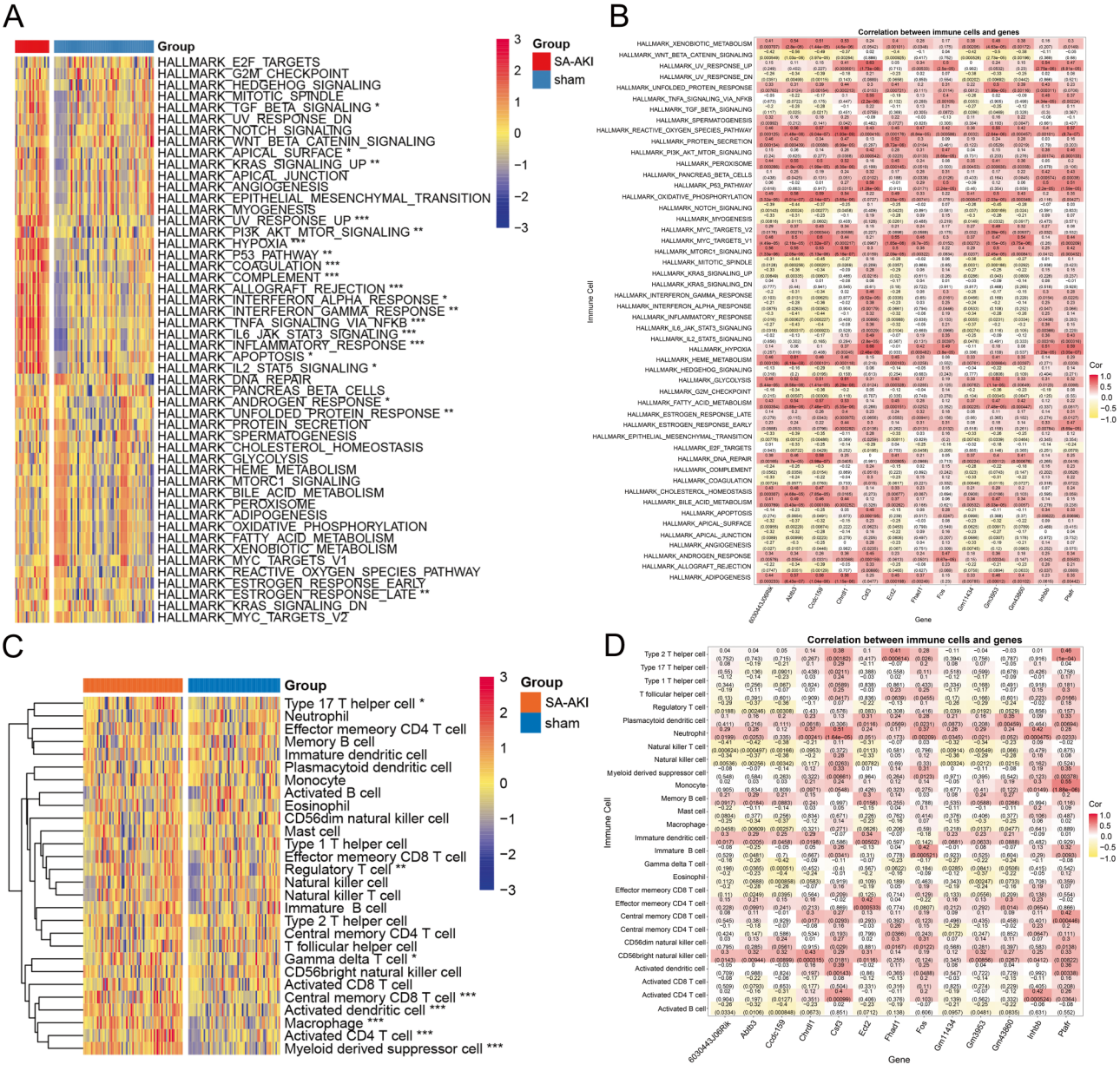

Fig. 6 Analysis of functional enrichment and immune infiltration of hub genes. (**A**) Based on HALLMARK gene set, single sample gene set enrichment analysis (ssGSEA) was performed to analyze the differences of biological processes between SA-AKI and sham samples. (**B**) The heat map of the correlations between the 13 hub genes and HALLMARK gene set scores. (**C**) ssGSEA was used to evaluate the infiltration of 28 kinds of immune cells in SA-AKI and sham samples. (**D**) The heat map of the correlations between the 13 hub genes and the infiltration of 28 immune cells. *$P < 0.05$, **$P < 0.01$, and ***$P < 0.001$

Acetaminophen, estradiol and (+)-JQ1 were chosen for further analysis. Molecular docking showed that estradiol and (+)-JQ1 have much better binding affinities with the hub targets, compared with those of acetaminophen (Fig. 7B). Molecular docking showed that, estradiol could form two hydrogen bonds with TYR-77 and ARG-14 amino acid residue of PTAFR, two hydrogen bonds with ARG-155 amino acid residue of CSF3, and one hydrogen bond with GLN-144 amino acid residue of CHRDL1; (+)-JQ1 could form two hydrogen bonds with TYR-1030 and ALA-1001 amino acid residues of PTAFR, one hydrogen bond with TYR-206 amino acid residue of CSF3, and two hydrogen bonds with SER-739 and GLU-652 amino acid residues of ECT2 (Fig. 7C). These results suggest that estradiol and (+)-JQ1 are candidate drugs to treat SA-AKI.

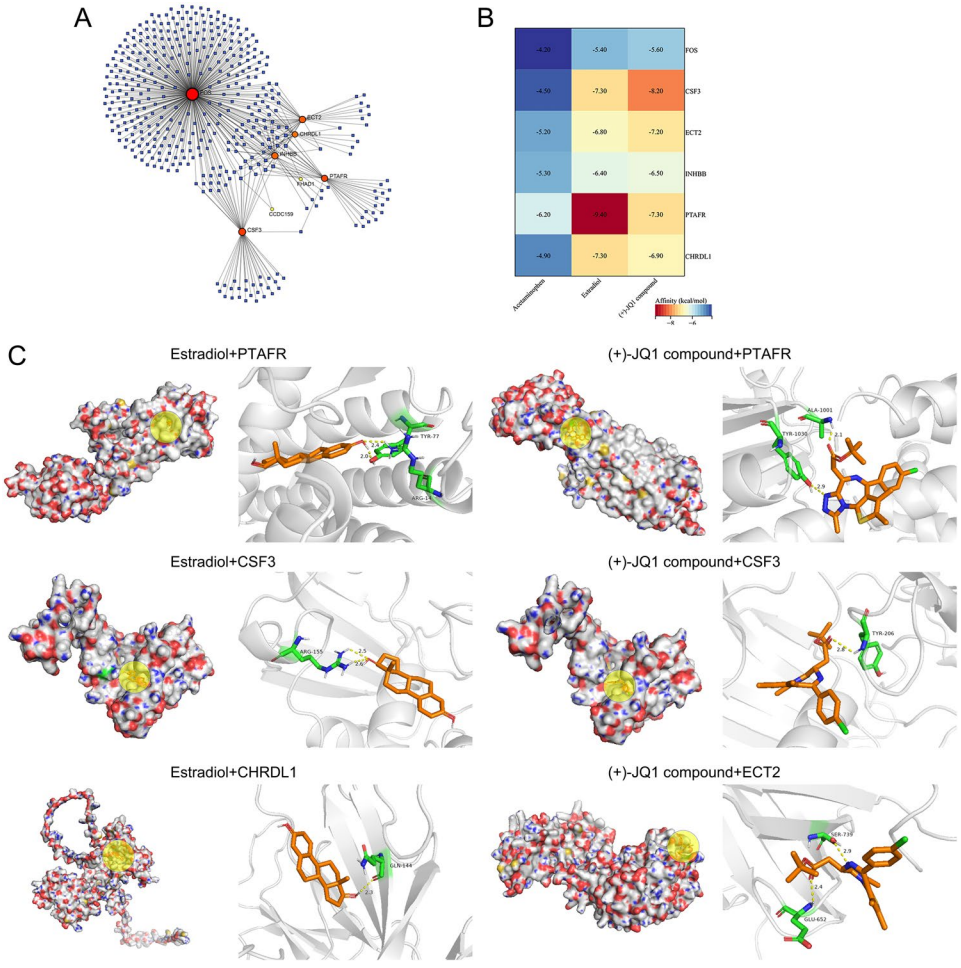

Fig. 7 The potential drugs targeting the hub targets. (**A**) Network diagram of the drugs targeting the hub targets in NetworkAnalyst database. The orange nodes represent the hub gene and the blue nodes represent the drug. (**B**) Heat map of molecular docking results. (**C**) 3D binding mode diagrams of estradiol and (+)-JQ1, and their targets. Orange represents the drug, green represents the amino acid residue, yellow dashed line represents the hydrogen bond, and gray represents the 3D structure of the protein

Table 3 The top 6 components targeting the hub targets in networkanalyst database

Drugs	Targets
Acetaminophen	CSF3, ECT2, FHAD1, FOS, INHBB, PTAFR
Silicon Dioxide	CSF3, ECT2, FHAD1, FOS, INHBB, PTAFR
Estradiol	CSF3, ECT2, FOS, INHBB, PTAFR
Aflatoxin B1	CHRDL1, ECT2, FOS, INHBB, PTAFR
potassium chromate(VI)	CHRDL1, ECT2, FOS, INHBB, PTAFR
(+)-JQ1 compound	CHRDL1, ECT2, FHAD1, FOS, PTAFR

The expression characteristics of hub genes in PBMCs of patients with SA-AKI and the regulatory effects of candidate drugs on renal tubular epithelial cells and vascular endothelial cells

To further verify the correlation between hub genes and SA-AKI, qRT-PCR was used to detect the expression of some hub genes in PBMCs of patients with SA-AKI and healthy controls. The results showed that the expression levels of ECT2 and CHRDL1 in SA-AKI patients were significantly lower than that in control group; the expression levels of PTAFR, CSF3 and FOS in SA-AKI patients were significantly higher than those in the control group (Fig. 8A), which was consistent with the in silico analysis. HK2 cells and HUVECs were stimulated by LPS, and CCK-8 assay showed that cell viability in the LPS treatment group was significantly lower than that in the control group, while estradiol and (+)-JQ1 compound treatment significantly increased the viability of HK-2 cells and HUVECs (Fig. 8B). Flow cytometry confirmed that estradiol and (+)-JQ1 significantly alleviated LPS-induced apoptosis of HK-2 cells and HUVECs (Fig. 8C). In addition, compared with LPS treatment group, treatment with estradiol and (+)-JQ1 significantly inhibited LPS-induced intracellular ROS and MDA accumulation (Fig. 8D&E).

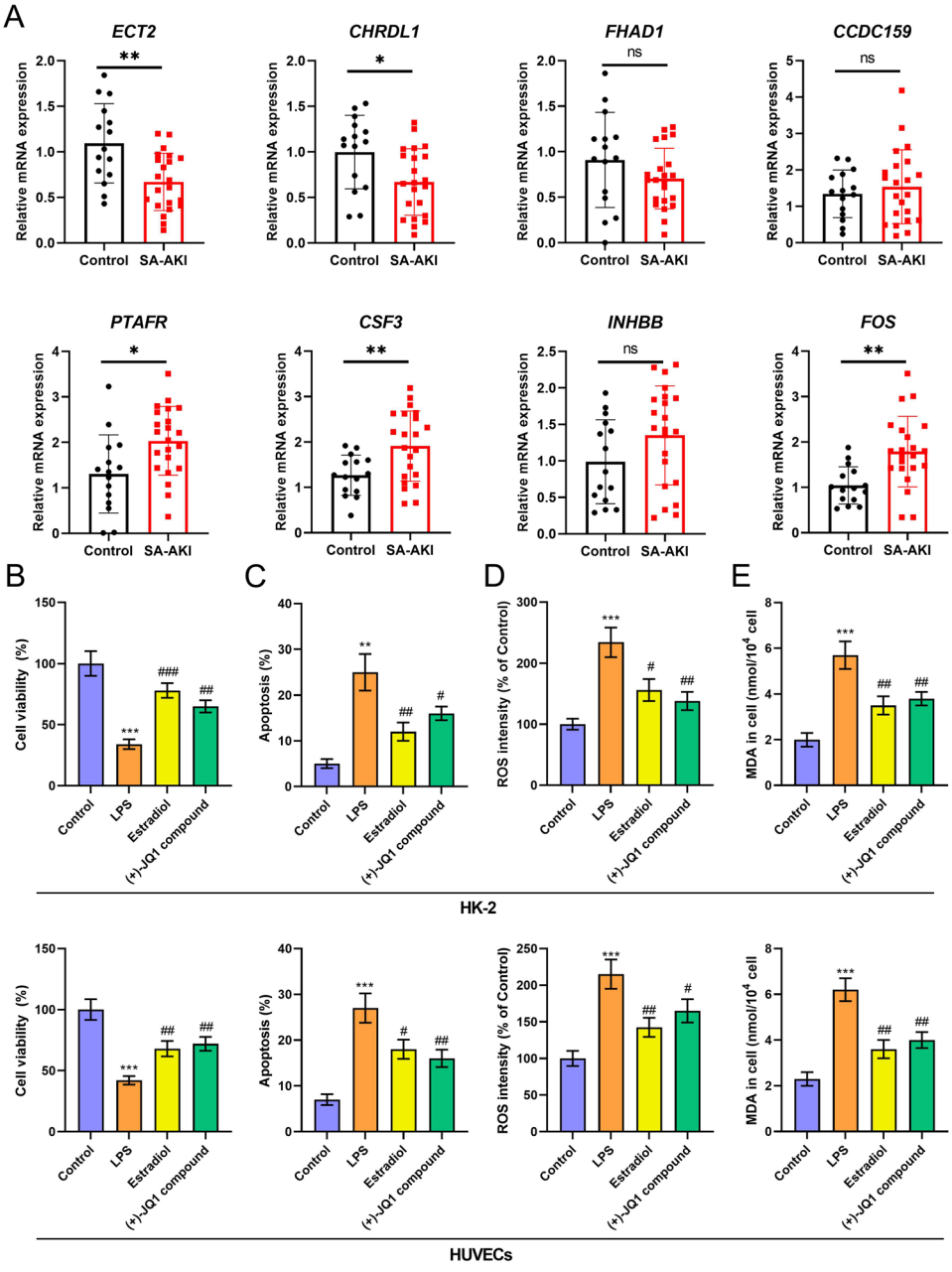

Fig. 8 The expression characteristics of hub genes in PBMCs of patients with SA-AKI and the regulatory effects of candidate drugs on renal tubular cells. (**A**) mRNA expressions of CCDC159, ECT2, CHRDL1, FOS, INHBB, CSF3, FHAD1 and PTAFR in peripheral blood mononuclear cells of 15 healthy controls and 22 SA-AKI patients were detected by qRT-PCR. (**B**) The viability of HK-2 cells and HUVECs in control group, lipopolysaccharide (LPS) treatment group, estradiol treatment group and (+)-JQ1 treatment group was detected by CCK-8 assay. (**C**) The apoptosis level of cells in different groups was detected by flow cytometry. (**D**-**E**) Reactive oxygen species (ROS) (**D**) and malonaldehyde (MDA) (**E**) levels in HK-2 cells and HUVECs of different treatment groups were assessed to evaluate the oxidative stress. **P* < 0.05 and ***P* < 0.01 vs. Control group; #*P* < 0.05, ##*P* < 0.01, and ###*P* < 0.001 vs. LPS group

Discussion

The incidence of SA-AKI varies between 25 and 75% depending on the the differences of cohort, severity of sepsis, and diagnostic criteria; in any case the occurrence of SA-AKI is associated with higher mortality and longer ICU stay [49, 50], and clarifying the mechanism of SA-AKI pathogenesis is of great significance to develop new treatment strategies and improve the patients' prognosis. The pathogenesis of SA-AKI is extremely complex and is influenced by multiple factors, including microvascular dysfunction, ROS formation, cell death, inflammation and metabolic reprogramming [51]. Exploring the pathogenesis of SA-AKI is of great significance to identify novel diagnostic biomarkers and therapeutic targets. After the innate immune system is activated, mast cells will rapidly release a large number of pro-inflammatory

factors, which can not only induce microvascular changes [52, 53], but also promote large recruitment of neutrophils, leading to AKI [54–56]. Activated neutrophils release NETs that stimulate macrophage recruitment and antigen presentation, thereby triggering cytotoxic T cell responses and enhancing renal tubular necrosis in AKI [57–59]. The studies mentioned above imply the importance of NETs in the pathogenesis of AKI, however few studies report the relationship between NETs and SA-AKI. In the present work, based on NETs-related genes, via unsupervised clustering, SA-AKI samples of mouse could be divided into two subgroups with distinct expression profiles of NETs-related genes. This suggests that NETs are involved in the pathogenesis of SA-AKI.

Interestingly, in the present work, bioinformatics analysis suggested that, OS were markedly associated with NETs in SA-AKI. Subsequently, 13 hub genes were screened, which were considered to be the crucial regulators of NETs formation and OS during SA-AKI, including *Ccdc159*, *Abtb3*, *Ect2*, *Chrdl1*, *Gm11434*, *6030443J06Rik*, *Gm43860*, *Gm3953*, *Fos*, *Inhbb*, *Csf3*, *Fhad1*, and *Ptafr*. Epithelial cell transforming 2 (ECT2) is involved in regulating vascular permeability during neutrophil exosmosis during acute inflammation [60]. In addition, ECT2 contributes to the tight junction function of renal epithelial cells and the maintenance of cell polarity, and the dysfunction of ECT2 leads to renal tubulointerstitial lesion [61]. In this study, ECT2 was found to be down-regulated in SA-AKI. Chordin like 1 (CHRDL1) is a specific inhibitor of bone morphogenetic proteins (BMPs), especially bone morphogenetic protein 4 (BMP4); BMPs play an important role in renal interstitial fibrosis and renal tubular injury in acute renal injury [62, 63]. Fos proto-oncogene, AP-1 transcription factor subunit (FOS) is a subunit of activating protein 1 (AP-1), belonging to the leucine zipper transcription factor family. The expression of FOS is up-regulated in kidney tissues of rats with AKI [64], which is consistent with the result of this study. FOS can directly modulate the transcription of inflammatory cytokines (such as TNF-α, IL-6 and IL-1β), and promote the pathogenesis of AKI [65]. Notably, a recent study reports that, FOS may be involved in the formation of NETs in myocardial infarction [66]. Inhibin subunit beta B (INHBB) encodes a member of the transforming growth factor β protein superfamily that plays a key role in the activation of NF-κB pathway [67]. Up-regulation of INHBB in renal tubular epithelial cells can activate interstitial fibroblasts and trigger fibrosis [68]. Colony stimulating factor 3 (CSF3) encodes a member of the IL-6 superfamily, which participates in the recruitment, adhesion and activation of neutrophils at the inflammatory site [69]. Previous studies have reported that inhibition of CSF3 pathway to reduce neutrophil accumulation may be a potentially effective way to improve the prognosis of SA-AKI [70, 71]. Platelet activating factor receptor (PTAFR) stimulates the infiltration of neutrophils, which impairs renal function [72, 73]. Our work suggested that these hub genes are pivotal in regulating the formation of NETs and OS in SA-AKI, and their biological functions and related molecular mechanism deserves to be further explored in the subsequent studies with biochemical assays. LASSO algorithm can compress the coefficients in the model so that some of the unimportant feature coefficients are reduced to zero. This advantage helps to simplify the model, reduce unnecessary features, and improve the interpretability of the model; in addition, LASSO also has the advantage of controlling the model to reduce the risk of overfitting and improve the model generalization ability [35]. In the present work, LASSO was used to identify the hub genes. It is worth noting that, other machine learning approaches may help find more potential regulators in SA-AKI, which may be tried in the following work.

Six compounds including acetaminophen, silicon dioxide, estradiol, aflatoxin B1, potassium chromate (VI) and (+)-JQ1 compound, targeted at least five hub targets. Silicon dioxide is inorganic compound and can not be absorbed by the body. Aflatoxin B1 and potassium chromate (VI) are toxic and can induce OS-related injury in kidney cells [74, 75]. Acetaminophen is one of the common analgesic and antipyretic drugs. Studies have shown that acetaminophen can reduce OS and inhibit excessive innate immune response in patients with sepsis [76–78]. However, excessive acetaminophen can lead to severe acute kidney injury [79], so it is necessary to be cautious in choosing Acetaminophen as treatment for SA-AKI patients. Estradiol can inhibit the accumulation of neutrophils and alleviate inflammatory response [80]. In addition, Estradiol can promote the regeneration of injured renal tubular cells, reduce apoptosis and fibrosis, and thus ameliorate the progression of AKI [81, 82]. (+)-JQ1 compound is an inhibitor of bromodomain and extraterminal domain (BET), which can reduce the expression of pro-inflammatory factors IL-1, IL-18β and IL-1 in patients with sepsis, and effectively attenuate the inflammatory damage induced by sepsis [83, 84]. In addition, (+)-JQ1 compound has shown promise in preclinical models of AKI and chronic kidney disease [85]. In this study, it was found that estradiol and (+)-JQ1, respectively, had good binding affinities with FOS, CSF3, ECT2, INHBB, PTAFR and CHRDL1. In vitro assays further showed that estradiol and (+)-JQ1 compound could significantly inhibit the OS in LPS-induced HK-2 cells and HUVECs, and increase cell viability. These data suggests that estradiol and (+)-JQ1 are promising drugs to treat SA-AKI. Of course, their safety and efficacy should be validated with clinical trials in the following studies.

There are some limitations to this study. First, the patients with SA-AKI rarely receive biopsy, so the present work only collected datasets of mouse model with SA-AKI. However in the patients' samples, the crucial genes, identified by in silico analysis, were indeed dysregulated, which validated the findings based on mice samples. Anyway, the roles of the hub genes in regulating NETs formation and OS, and in modulating the pathogenesis of SA-AKI requires further validation with animal models and clinical data. Secondly, even though in the present work we preliminarily proved the protective effects of estradiol and (+)-JQ1 on renal tubular epithelial cells, the current data are insufficient to clarify the effects of the two drugs on the formation of NETs, which should be explored in the following work. Additionally, injury of glomerular cells and renal interstitial cells are also involved in SA-AKI, the regulatory effects of estradiol and (+)-JQ1 on these cells should be further investigated in the future. Last but not least, increasing studies have shown that metabolic alterations are associated with organ injury in septic shock [86, 87], and there is a reciprocal regulation mechanism between NETs formation and metabolic alteration [88]. In the following studies, the potential roles of hub genes and (+)-JQ1 in regulating metabolic alterations in SA-AKI deserves further investigation.

Conclusion

Formation of NETs contributes to the pathogenesis of SA-AKI, which may be associated with OS. Multiple hub genes, including ECT2, CHRDL1, PTAFR, CSF3 and FOS, are potential regulators of the formation of NETs and OS in SA-AKI. Additionally, estradiol and (+)-JQ1 are promising drugs to ameliorate SA-AKI by targeting these hub targets.

Supplementary Information

The online version contains supplementary material available at https://doi.org/10.1186/s12882-025-04126-y.

Supplementary Material 1: Merging GSE33118 and GSE26440 datasets. (A-B) sva algorithm was used to remove batch effect of GSE33118 and GSE26440 datasets, and principal component analysis (PCA) was used to show the original data distribution pattern (A) and mixed data distribution pattern (B)

Acknowledgement
None.

Author contributions
Conceived and designed the experiments: Xia Zhongyuan & Sun Qian; Performed the in silico analysis: Tang Shaoqun & Yu Xi; Performed the experiments: Tang Shaoqun, Wang Wei, Luo Yaru, Lei Shaoqing, Qiu Zhen & Yang Yanlin; Analyzed the data: Tang Shaoqun, Yu Xi & Wang Wei; Drafted the paper: Tang Shaoqun. Reviewed the manuscript: Xia Zhongyuan & Sun Qian. All authors read and approved the final manuscript.

Funding
This study was supported by grants from the National Natural Science Foundation of China (82372188, 82202408) and the Hubei Province Natural Science Foundation (No. 2023AFB821).

Data availability
Related codes in the present work are available from https://github.com/tangshaoqun-R/SAKI. Data used to support the findings of this study are also available from the corresponding author upon request.

Declarations

Ethical approval
This study is approved by the Research Ethics Committee of Renmin Hospital of Wuhan University.

Consent to participate
All of the patients enrolled in this study agree to participate in this work.

Competing interests
The authors declare no competing interests.

Author details
[1]Department of Anesthesiology, Renmin Hospital of Wuhan University, Wuhan, Hubei 430060, China

Received: 10 November 2024 / Accepted: 14 April 2025
Published online: 14 May 2025

References

1. Gavelli F, Castello LM, Avanzi GC. Management of sepsis and septic shock in the emergency department. Intern Emerg Med. 2021;16(6):1649–61.
2. Manzoor A, Umme-e-Aiman M. Maryam. Understanding COVID-19: an overview of the virus, variants, vaccines, and treatment strategies. Diagnostics Ther. 2024;3(1):9–19.
3. Fleischmann-Struzek C, Mellhammar L, Rose N, et al. Incidence and mortality of hospital- and ICU-treated sepsis: results from an updated and expanded systematic review and meta-analysis. Intensive Care Med. 2020;46(8):1552–62.
4. Bagshaw SM, Lapinsky S, Dial S, et al. Acute kidney injury in septic shock: clinical outcomes and impact of duration of hypotension prior to initiation of antimicrobial therapy. Intensive Care Med. 2009;35(5):871–81.
5. Bagshaw SM, Uchino S, Bellomo R, et al. Septic acute kidney injury in critically ill patients: clinical characteristics and outcomes. Clin J Am Soc Nephrology: CJASN. 2007;2(3):431–9.
6. Poston JT, Koyner JL. Sepsis associated acute kidney injury. BMJ. 2019;364:k4891.
7. Hidalgo A, Libby P, Soehnlein O, et al. Neutrophil extracellular traps: from physiology to pathology. Cardiovascular Res. 2022;118(13):2737–53.
8. Shen XF, Cao K, Jiang JP, Guan WX, Du JF. Neutrophil dysregulation during sepsis: an overview and update. J Cell Mol Med. 2017;21(9):1687–97.
9. Li RHL, Tablin F. A comparative review of neutrophil extracellular traps in Sepsis. Front Veterinary Sci. 2018;5:291.
10. Chen L, Zhao Y, Lai D, et al. Neutrophil extracellular traps promote macrophage pyroptosis in sepsis. Cell Death Dis. 2018;9(6):597.
11. Sun S, Duan Z, Wang X, et al. Neutrophil extracellular traps impair intestinal barrier functions in sepsis by regulating TLR9-mediated Endoplasmic reticulum stress pathway. Cell Death Dis. 2021;12(6):606.
12. Chen Z, Zhang H, Qu M, et al. Review: the emerging role of neutrophil extracellular traps in Sepsis and Sepsis-Associated thrombosis. Front Cell Infect Microbiol. 2021;11:653228.
13. Alsabani M, Abrams ST, Cheng Z, et al. Reduction of NETosis by targeting CXCR1/2 reduces thrombosis, lung injury, and mortality in experimental human and murine sepsis. Br J Anaesth. 2022;128(2):283–93.
14. Kaplan MJ, Radic M. Neutrophil extracellular traps: double-edged swords of innate immunity. J Immunol (Baltimore Md: 1950). 2012;189(6):2689–95.
15. Colón DF, Wanderley CW, Franchin M, et al. Neutrophil extracellular traps (NETs) exacerbate severity of infant sepsis. Crit Care (London England). 2019;23(1):113.

16. Ni Y, Hu BC, Wu GH, et al. Interruption of neutrophil extracellular traps formation dictates host defense and tubular HOXA5 stability to augment efficacy of anti-Fn14 therapy against septic AKI. Theranostics. 2021;11(19):9431–51.
17. Okeke EB, Louttit C, Fry C, et al. Inhibition of neutrophil elastase prevents neutrophil extracellular trap formation and rescues mice from endotoxic shock. Biomaterials. 2020;238:119836.
18. Ow CPC, Trask-Marino A, Betrie AH et al. Targeting oxidative stress in septic acute kidney injury: from theory to practice. J Clin Med. 2021;10(17).
19. Balkrishna A, Sinha S, Kumar A, et al. Sepsis-mediated renal dysfunction: pathophysiology, biomarkers and role of phytoconstituents in its management. Biomed pharmacotherapy = Biomedecine Pharmacotherapie. 2023;165:115183.
20. Rui Y, Li S, Luan F et al. Several alkaloids in Chinese herbal medicine exert protection in acute kidney injury: focus on mechanism and target analysis. Oxid Med Cell Longev. 2022;2022:2427802.
21. Zhong D, Pan Y, Fan H, et al. Protective effect of Salidroside on acute kidney injury in Sepsis by inhibiting oxidative stress, mitochondrial damage, and cell apoptosis. Biol Pharm Bull. 2024;47(9):1550–6.
22. Manoj H, Gomes SM, Thimmappa PY et al. Cytokine signalling in formation of neutrophil extracellular traps: implications for health and diseases. Cytokine Growth Factor Rev. 2024;9:S1359-6101(24)00102-3.
23. Wigerblad G, Kaplan MJ. Neutrophil extracellular traps in systemic autoimmune and autoinflammatory diseases. Nat Rev Immunol. 2023;23(5):274–88.
24. Leek JT, Storey JD. Capturing heterogeneity in gene expression studies by surrogate variable analysis. PLoS Genet. 2007;3:e161.
25. Zhang Y, Guo L, Dai Q et al. A signature for pan-cancer prognosis based on neutrophil extracellular traps. J Immunother Cancer. 2022;10(6).
26. Wilkerson MD, Hayes DN. ConsensusClusterPlus: a class discovery tool with confidence assessments and item tracking. Bioinformatics. 2010;26(12):1572–3.
27. Diboun I, Wernisch L, Orengo CA, Koltzenburg M. Microarray analysis after RNA amplification can detect pronounced differences in gene expression using Limma. BMC Genomics. 2006;7:252.
28. Wickham H. ggplot2, WIREs Comput Stat. 2011;3:180–185.
29. Li M, Mao S, Li L, Wei M. Hypoxia-related LncRNAs signature predicts prognosis and is associated with immune infiltration and progress of head and neck squamous cell carcinoma. Biochem Biophys Rep. 2022;31:101304.
30. Langfelder P, Horvath S. WGCNA: an R package for weighted correlation network analysis. BMC Bioinformatics. 2008;9:559.
31. Safran M, Dalah I, Alexander J, et al. GeneCards version 3: the human gene integrator. Database (Oxford). 2010;2010:baq020.
32. Hänzelmann S, Castelo R, Guinney J. GSVA: gene set variation analysis for microarray and RNA-seq data. BMC Bioinformatics. 2013;14:7.
33. Yu G, Wang LG, Han Y, He QY. ClusterProfiler: an R package for comparing biological themes among gene clusters. OMICS. 2012;16(5):284–7.
34. Liberzon A, Subramanian A, Pinchback R, Thorvaldsdóttir H, Tamayo P, Mesirov JP. Molecular signatures database (MSigDB) 3.0. Bioinformatics. 2011;27(12):1739–40.
35. Yang C, Delcher C, Shenkman E, Ranka S. Machine learning approaches for predicting high cost high need patient expenditures in health care. Biomed Eng Online. 2018;17(Suppl 1):131.
36. Xu Y, Lin C, Han C, et al. Development of a prognostic nomogram and risk stratification system for elderly patients with esophageal squamous cell carcinoma undergoing definitive radiotherapy: a multicenter retrospective analysis (3JECROG R-03 A). BMC Cancer. 2025;25(1):40.
37. Peterson W, Birdsall T, Fox W. The theory of signal detectability. Trans IRE Prof Group Inf Theory. 1954;4:171–212.
38. Huang J, Ling CX. Using AUC and accuracy in evaluating learning algorithms. IEEE Trans Knowl Data Eng. 2025;17(3):299–310.
39. Zhou G, Soufan O, Ewald J, Hancock REW, Basu N, Xia J. NetworkAnalyst 3.0: a visual analytics platform for comprehensive gene expression profiling and meta-analysis. Nucleic Acids Res. 2019;47(W1):W234–41.
40. Davis AP, Murphy CG, Johnson R, et al. The comparative toxicogenomics database: update 2013. Nucleic Acids Res. 2013;41(Database issue):D1104–14.
41. UniProt Consortium. UniProt: the universal protein knowledgebase in 2025. Nucleic Acids Res. 2025;53(D1):D609–17.
42. Trott O, Olson AJ. AutoDock Vina: improving the speed and accuracy of docking with a new scoring function, efficient optimization, and multithreading. J Comput Chem. 2010;31(2):455– 61.
43. Seeliger D, de Groot BL. Ligand Docking and binding site analysis with PyMOL and Autodock/Vina. J Comput Aided Mol Des. 2010;24(5):417–22.
44. Singer M, Deutschman CS, Seymour CW et al. The third international consensus definitions for Sepsis and septic shock (Sepsis-3). JAMA. 2016;315(8):801– 10.
45. Chen WY, Cai LH, Zhang ZH et al. The timing of continuous renal replacement therapy initiation in sepsis-associated acute kidney injury in the intensive care unit: the CRTSAKI study (Continuous RRT timing in Sepsis-associated AKI in ICU): study protocol for a multicentre, randomised controlled trial. BMJ Open, 11(2), 2021, e040718.
46. Riedhammer C, Halbritter D, Weissert R. Peripheral blood mononuclear cells: isolation, freezing, thawing, and, culture. Methods Mol Biol. 2016;1304:53–61.
47. Kong C, Zhu Y, Xie X, Wu J, Qian M. Six potential biomarkers in septic shock: a deep bioinformatics and prospective observational study. Front Immunol. 2023;14:1184700.
48. Sun M, Li J, Mao L, et al. p53 deacetylation alleviates Sepsis-Induced acute kidney injury by promoting autophagy. Front Immunol. 2021;12:685523.
49. Legrand M, Bagshaw SM, Bhatraju PK. Sepsis-associated acute kidney injury: recent advances in enrichment strategies, sub-phenotyping and clinical trials. Crit Care. 2024;28(1):92.
50. Zarbock A, Nadim MK, Pickkers P, et al. Sepsis-associated acute kidney injury: consensus report of the 28th acute disease quality initiative workgroup. Nat Rev Nephrol. 2023;19(6):401–17.
51. Gómez H, Kellum JA. Sepsis-induced acute kidney injury. Curr Opin Crit Care. 2016;22(6):546– 53.
52. Oschatz C, Maas C, Lecher B, et al. Mast cells increase vascular permeability by heparin-initiated Bradykinin formation in vivo. Immunity. 2011;34(2):258–68.
53. Cho C, Nguyen A, Bryant KJ, O'Neill SG, McNeil HP. Prostaglandin D2 metabolites as a biomarker of in vivo mast cell activation in systemic mastocytosis and rheumatoid arthritis. Immun Inflamm Dis. 2016;4(1):64– 9.
54. Mihlan M, Wissmann S, Gavrilov A, et al. Neutrophil trapping and nexocytosis, mast cell-mediated processes for inflammatory signal relay. Cell. 2024;187(19):5316–e3528.
55. Summers SA, Chan J, Gan PY, et al. Mast cells mediate acute kidney injury through the production of TNF. J Am Soc Nephrology: JASN. 2011;22(12):2226–36.
56. Madjene LC, Danelli L, Dahdah A, et al. Mast cell chymase protects against acute ischemic kidney injury by limiting neutrophil hyperactivation and recruitment. Kidney Int. 2020;97(3):516–27.
57. Nakazawa D, Kumar SV, Marschner J, et al. Histones and neutrophil extracellular traps enhance tubular necrosis and remote organ injury in ischemic AKI. J Am Soc Nephrology: JASN. 2017;28(6):1753–68.
58. Jorch SK. P. Kubes 2017 An emerging role for neutrophil extracellular traps in noninfectious disease. Nat Med 23 3 279–87.
59. Lande R, Ganguly D, Facchinetti V, et al. Neutrophils activate plasmacytoid dendritic cells by releasing self-DNA-peptide complexes in systemic lupus erythematosus. Sci Transl Med. 2011;3(73):73ra19.
60. Heemskerk N, Schimmel L, Oort C, et al. F-actin-rich contractile endothelial pores prevent vascular leakage during leukocyte diapedesis through local RhoA signalling. Nat Commun. 2016;7:10493.
61. Izu A, Sugimoto K, Fujita S, et al. Nonfunction of the ECT2 gene May cause renal tubulointerstitial injury leading to focal segmental glomerulosclerosis. Clin Exp Nephrol. 2012;16(6):875–82.
62. Lin J, Patel SR, Cheng X, et al. Kielin/chordin-like protein, a novel enhancer of BMP signaling, attenuates renal fibrotic disease. Nat Med. 2005;11(4):387–93.
63. Larman BW, Karolak MJ, Lindner V, Oxburgh L. Distinct bone morphogenetic proteins activate indistinguishable transcriptional responses in nephron epithelia including Notch target genes. Cell Signal. 2012;24(1):257–64.
64. Xu J, Xu Y. Identifying of miRNA-mRNA regulatory networks associated with acute kidney injury by weighted gene Co-Expression network analysis. Int J Gen Med. 2022;15:1853–64.
65. Zhang C, Ma P, Zhao Z, et al. miRNA–mRNA regulatory network analysis of mesenchymal stem cell treatment in cisplatin–induced acute kidney injury identifies roles for miR–210/Serpine1 and miR–378/Fos in regulating inflammation. Mol Med Rep. 2019;20(2):1509–22.
66. Li X, Wu W, He H, et al. Analysis and validation of hub genes in neutrophil extracellular traps for the long-term prognosis of myocardial infarction. Gene. 2024;914:148369.
67. Jin Y, Cai Q, Wang L, et al. Paracrine activin B-NF-κB signaling shapes an inflammatory tumor microenvironment in gastric cancer via fibroblast reprogramming. J Experimental Clin cancer Research: CR. 2023;42(1):269.
68. Sun Y, Cai H, Ge J, et al. Tubule-derived INHBB promotes interstitial fibroblast activation and renal fibrosis. J Pathol. 2022;256(1):25–37.

69. Wilhelmsen K, Mesa KR, Prakash A, Xu F, Hellman J. Activation of endothelial TLR2 by bacterial lipoprotein upregulates proteins specific for the neutrophil response. Innate Immun. 2012;18(4):602–16.
70. Wang H, Tumes DJ, Hercus TR, et al. Blocking the human common beta subunit of the GM-CSF, IL-5 and IL-3 receptors markedly reduces hyperinflammation in ARDS models. Cell Death Dis. 2022;13(2):137.
71. Kang ZY, Huang QY, Zhen NX, et al. Heterogeneity of immune cells and their communications unveiled by transcriptome profiling in acute inflammatory lung injury. Front Immunol. 2024;15:1382449.
72. Latchoumycandane C, Nagy LE, McIntyre TM. Myeloperoxidase formation of PAF receptor ligands induces PAF receptor-dependent kidney injury during ethanol consumption. Free Radic Biol Med. 2015;86:179–90.
73. Latchoumycandane C, Hanouneh M, Nagy LE, McIntyre TM. Inflammatory PAF receptor signaling initiates Hedgehog signaling and kidney fibrogenesis during ethanol consumption. PLoS One. 2015;10(12):e0145691.
74. Dlamini NZ, Somboro AM, Amoako DG, et al. Toxicogenicity and mechanistic pathways of aflatoxin B1 induced renal injury. Environ Toxicol. 2021;36(9):1857–72.
75. Miyajima H, Hewitt WR, Coté MG, Plaa GL. Relationships between histological and functional indices of acute chemically induced nephrotoxicity. Fundamental Appl Toxicology: Official J Soc Toxicol. 1983;3(6):543–51.
76. Husain AA, Martin GS. What is old is new again: acetaminophen as a novel approach to treating sepsis. Crit Care Med. 2015;43(3):698–9.
77. Janz DR, Bastarache JA, Rice TW et al. Randomized, placebo-controlled trial of acetaminophen for the reduction of oxidative injury in severe sepsis: the acetaminophen for the reduction of oxidative injury in severe sepsis trial. Crit Care Med. 2015;43(3):534–41.
78. Ware LB, Files DC, Fowler A, et al. Acetaminophen for prevention and treatment of organ dysfunction in critically ill patients with sepsis: the ASTER randomized clinical trial. JAMA. 2024;332(5):390–400.
79. Xiong C, Jia Y, Wu X, et al. Early postoperative acetaminophen administration and severe acute kidney injury after cardiac surgery. Am J Kidney Diseases: Official J Natl Kidney Foundation. 2023;816:675–e831.
80. Vermillion MS, Ursin RL, Attreed SE, Klein SL. Estriol reduces pulmonary immune cell recruitment and inflammation to protect female mice from severe influenza. Endocrinology. 2018;159(9):3306–20.
81. Wu CC, Chang CY, Chang ST, Chen SH. 17β-Estradiol accelerated renal tubule regeneration in male rats after ischemia/reperfusion-induced acute kidney injury. Shock. 2016;46(2):158–63.
82. Ren L, Li F, Di Z, et al. Estradiol ameliorates acute kidney Ischemia-Reperfusion injury by inhibiting the TGF-βRI-SMAD pathway. Front Immunol. 2022;13:822604.
83. Chen L, Zhong X, Cao W, et al. JQ1 as a BRD4 inhibitor blocks inflammatory Pyroptosis-Related acute Colon injury induced by LPS. Front Immunol. 2021;12:609319.
84. Zhong X, Chen Z, Wang Y, et al. JQ1 attenuates neuroinflammation by inhibiting the inflammasome-dependent canonical pyroptosis pathway in SAE. Brain Res Bull. 2022;189:174–83.
85. Saiz ML, Lozano-Chamizo L, Florez AB, et al. BET inhibitor nanotherapy halts kidney damage and reduces chronic kidney disease progression after ischemia-reperfusion injury. Biomed Pharmacother. 2024;174:116492.
86. Pandey S, Adnan Siddiqui M, Azim A, Trigun SK, Sinha N. Serum metabolic profiles of septic shock patients based upon co-morbidities and other underlying conditions. Mol Omics. 2021;17(2):260–76.
87. Huen SC. Metabolism as disease tolerance: implications for Sepsis-Associated acute kidney injury. Nephron. 2022;146(3):291–4.
88. Zhu L, Zheng Q, Liu X, et al. HMGB1 lactylation drives neutrophil extracellular trap formation in lactate-induced acute kidney injury. Front Immunol. 2025;15:1475543.

Publisher's note